Clays and Clay Minerals, Vol. 33, No. 3, 237–243, 1985.

SMALL-ANGLE X-RAY POWDER DIFFRACTION, MORPHOLOGY, AND STRUCTURE OF ALLOPHANE AND IMOGOLITE

S. J. VAN DER GAAST
Netherlands Institute for Sea Research, P.O. Box 59, Texel, The Netherlands

K. WADA, S.-I. WADA, AND Y. KAKUTO
Faculty of Agriculture, Kyushu University 46, Fukuoka 812, Japan

Abstract—Small-angle X-ray powder diffraction analyses and high-resolution electron microscopy of allophane samples (SiO_2/Al_2O_3 ratio, 1.12 to 1.68) showed that allophanes consist of nearly identical spherical particles with diameters of about 40 Å and retain their characteristic "hollow" spherical morphology at different ambient moisture and even after dehydroxylation by heating at 500° to 600°C. Unheated allophane samples gave another X-ray powder diffraction band whose maximum position varied from 12.3 to 14.5 Å depending on their SiO_2/Al_2O_3 ratio. The appearance of this band may denote some long-range ordering in the structure of allophane. Unlike the spherical particles of allophane, the tube unit of imogolite collapsed on dehydroxylation. This observation suggests that imogolite and allophane are different in their framework structures and that a Si- or Si(Al)-tetrahedral sheet rather than an Al-octahedral sheet constitutes the framework structure of allophane, irrespective of its SiO_2/Al_2O_3 ratio.

要約 ―アロフエン試料 (SiO_2/Al_2O_3比，1.12 ないし 1.68) の小角X線粉末回折と高分解能電子顕微鏡観察は，アロフエンが直径約 40Å のほとんど同様の球状粒子より成り，異なる水分ふん囲気中，及び 500 ないし 600°C 加熱による脱 OH 反応後でさえも，その特徴的な "中空" 球状の形態を維持することを示した。加熱しなかったアロフエン試料はその極大位置が 12.3 から 14.5Å に試料のSiO_2/Al_2O_3比によって変化するもう一つのX線粉末回折帯を与えた。この回折帯の出現はアロフエン構造内になんらかの広範囲に及ぶ規則性が存在することを示すものであろう。球状のアロフエン粒子と異なり，イモゴライトの管状単位は脱 OH 反応によって崩壊した。この観察は，イモゴライトとアロフエンでは骨格構造に差異があり，アロフエンの骨格構造は，そのSiO_2/Al_2O_3比に関係なく，Al- 八面体シートよりはむしろ Si あるいは Si(Al)- 四面体シートより成ることを示唆している。

Key Words—Allophane, Dehydroxylation, Imogolite, Infrared spectroscopy, Morphology, Small angle scattering.

INTRODUCTION

Allophanes are present in many soils derived from volcanic ash and weathered pumices. High-resolution electron microscopy has shown that allophanes consist of "hollow" spherical particles or polyhedra with external diameters of 55 Å (Kitagawa, 1971) or 35 to 50 Å (Henmi and Wada, 1976). In the electron microscope, allophane particles are exposed to high vacuum and electron bombardment; whether these conditions affect the morphology has not been confirmed. If allophane consists of nearly identical spherical particles as indicated by the electron microscopy, however, they should give a small-angle X-ray powder diffraction (XRD) band characteristic of such systems (Guinier, 1963). In the first part of the present paper, the small-angle X-ray powder diffraction (XRD) analyses of four allophane samples with different SiO_2/Al_2O_3 molar ratios are reported. The analyses were carried out on unheated and heated samples at 200° to 600°C and equilibrated at 0 and 100% relative humidity (r.h.) using the method developed by van der Gaast and Vaars (1981). The analyses provided information about the size and shape of allophane particles and their internal structure.

In the second part of the paper similar analyses are reported for a single imogolite sample. Imogolite is a unique paracrystalline clay mineral that consists of bundles of a long tube unit with an external diameter of about 20 Å (Wada *et al.*, 1970). It occurs with allophane in many soils derived from volcanic ash and weathered pumices. Cradwick *et al.* (1972) proposed a structure for the tube unit that consists of a single continuous gibbsite sheet with its inner-hydroxyl surface replaced by O_3SiOH groups. This proposed structure accounts for most features of the electron diffraction patterns, the morphology, and the chemical composition of imogolite. There remain, however, problems regarding the interpretation of some of the XRD bands in relation to the size and arrangement of the tube at different ambient humidities and temperatures.

Finally an argument exists about whether the wall of the allophane particles consists of a defect kaolin layer (Wada and Wada, 1977) or a defect imogolite layer (Parfitt *et al.*, 1980; Parfitt and Henmi, 1980). The small-angle XRD analyses of heated allophane and imogolite samples brought fresh light to bear on this question.

Copyright © 1985, The Clay Minerals Society

https://doi.org/10.1346/CCMN.1985.0330310 Published online by Cambridge University Press

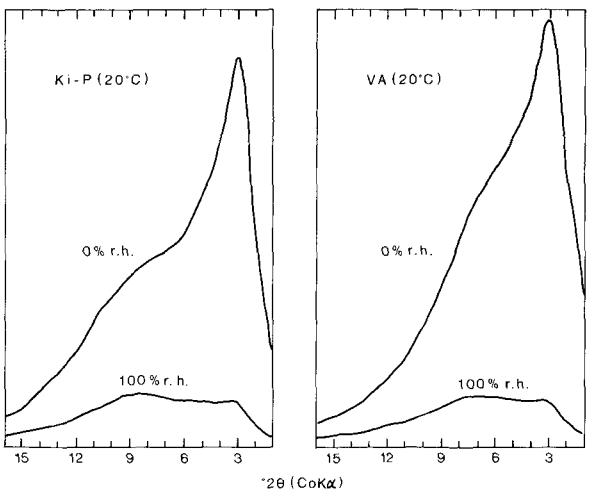


Figure 1. X-ray powder diffraction patterns of allophanes (Ki-P and VA) equilibrated at 0 and 100% relative humidity, respectively.

MATERIALS AND METHODS

Allophane samples were separated from three weathered pumices collected at Kitakami, Iwate (Ki-P); Kurayoshi, Tottori (Ku-P); and Choyo, Kumamoto (PA-P); and from one weathered volcanic ash collected at Choyo, Kumamoto (VA), Japan. One imogolite sample (Ki-G) was collected from gel films present in the Kitakami pumice bed. All samples were treated with H_2O_2 to remove organic matter and dispersed at pH 4 for the Ki-P, Ku-P, and Ki-G samples, and at pH 10 for the PA-P and VA samples. Clay-size fractions (<0.2 μm) were collected by centrifugation, followed by flocculation with NaCl, water washing, acetone washing, and air drying. Electron microscopy showed that the collected clay samples consisted of nearly pure allophane or imogolite. The SiO_2/Al_2O_3 molar ratio of the samples Ki-P, Ku-P, PA-P, and VA allophane samples were 1.12, 1.38, 1.67, and 1.68, respectively.

For the XRD analyses, the samples suspended in water were suctioned through polished, porous ceramic plates to produce flat aggregates and dried at room temperature. The XRD analyses were carried out using a wide angle PW1050/25 goniometer (Philips) in combination with a broad focus Co tube (CoKα), a graphite monochromator, and a vacuum-helium device. The instrument used earlier by van der Gaast and Vaars (1981) was improved with a self-developed, computer-aided divergence slit system that enabled constant sample-area irradiation independent of the angle of incidence and accurate goniometer alignment. The goniometer radius was increased from 173 mm to 214 mm. To avoid parasitic scattering at small angles, a 0.1-mm receiving slit and a ½°-antiscatter slit were used. The relative humidity in the sample chamber was kept constant at the desired values with a flow of moist or dry helium from a self-developed humidity generator. The humidity monitoring part of this device consisted of a Humicap HMI 12 with a HMP 14 probe that controlled the humidity within the accuracy of 1%. The XRD patterns were recorded in stepscan mode with a counting time of 4 sec/0.02°2θ for CoKα and stored on floppy disc. The recorded XRD patterns were corrected with the Lorentz polarization factor (MacEwan *et al.*, 1961) and for the irradiated volume. A Ludox silica sample (grade, SM; particle size 70–80 Å) was used as reference material for the XRD analyses.

RESULTS AND DISCUSSION

Allophane

As illustrated in Figure 1 for the Ki-P and VA samples, the unheated allophane samples equilibrated at 0% r.h. gave a fairly well defined XRD band with maximum at 2.95 to 3.10°2θ (CoKα) which was overlapped possibly by another broad band with maximum at 7.0 to 9.0°2θ (Table 1). At 100% r.h., a remarkable decrease in diffracted X-ray intensity occurred particularly for the first band showing a broadening toward the second band (Figure 1).

The relative enhancement of the first band at 0% r.h. suggests that it arose from the interference between the neighboring allophane particles. The latter interference increased with the removal of intervening water molecules. The magnitude of the distance between the

Table 1. The positions of the first and second X-ray powder diffraction bands from allophanes equilibrated at 0 and 100% relative humidity.

		First band[1] (°2θ; CoKα)		Second band[1] (°2θ; CoKα)	
		Relative humidity (%)		Relative humidity (%)	
Sample[2]	SiO_2/Al_2O_3 ratio	100	0	100	0
Ki-P	1.12	3.1 (33)	3.0 (34)	8.3 (12.4)	9.0 (11.4)
Ku-P	1.38	3.1 (33)	2.95 (30)	8.0 (12.8)	8.5 (12.1)
Pa-P	1.67	3.3 (31)	3.05 (33)	7.4 (13.9)	7.5 (13.7)
VA	1.68	3.45 (30)	3.1 (33)	7.1 (14.4)	7.0 (14.7)

[1] Figures in parentheses are d-spacings calculated using the Bragg formula (Å).
[2] See text for locations.

https://doi.org/10.1346/CCMN.1985.0330310 Published online by Cambridge University Press

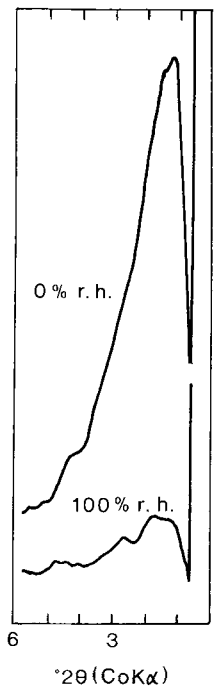


Figure 2. X-ray powder diffraction patterns of Ludox silica at 0 and 100% relative humidity, respectively.

neighboring particles that corresponds to their diameter d_m was estimated using the theory of small-angle X-ray scattering for dense systems of identical spherical particles (Guinier, 1963). As for monatomic liquids, the following relation exists:

$$2 \sin \theta/\lambda = 1.1 \text{ to } 1.2/d_m, \quad (1)$$

where θ is the Bragg glancing angle and λ the wavelength of the X-rays. The estimated d_m value of 37.5 to 41 Å is in agreement with the external diameter of the allophane spherical particles, i.e., 35 to 50 Å (Henmi and Wada, 1976). The 2θ, and hence the d_m, values did not differ between the samples with different SiO_2/Al_2O_3 ratios (Table 1). This relationship was also observed by electron microscopy (Henmi and Wada, 1976). At 100% r.h. the first band maximum slightly shifted toward the high-angle side for the PA and VA samples with higher SiO_2/Al_2O_3 ratios (Table 1). This shift probably resulted from the overlapping with the broad second band and does not indicate a variation in the size and morphology of allophane particles with the ambient moisture coupled with a variation of its chemical composition. The decrease of diffracted XRD intensity suggests an intervening effect of water present between the allophane particles that caused irregular distances compared with the more regular packing of the particles at 0% r.h. A similar observation was made for a reference Ludox silica sample. It gave a fairly well defined XRD band with maximum at 1.3°2θ (CoKα)

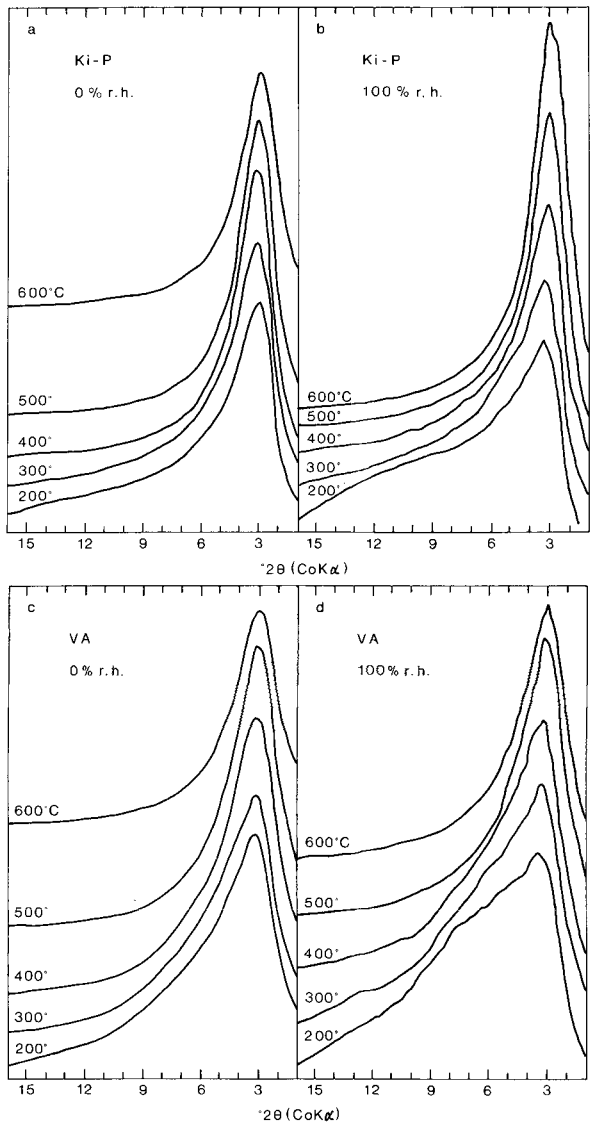


Figure 3. X-ray powder diffraction patterns of allophanes (Ki-P and VA) heated at 200°, 300°, 400°, 500°, and 600°C, and equilibrated at 0 and 100% relative humidity, respectively.

at 0% r.h. (Figure 2). The estimated d_m value was 87 to 95 Å. The diameter of most particles observed on the electron micrographs was in the range from 86 to 114 Å.

The occurrence of a strong XRD band for allophane that corresponds to the second band in the present study was recorded by Brown (1980) together with six other XRD bands at higher angles. Unlike the first XRD band, the 2θ value of the second band varied with the SiO_2/Al_2O_3 ratio of allophane samples both at 0 and 100% r.h. (Table 1). Thus, the band likely arose from some long-range ordering in the structure

https://doi.org/10.1346/CCMN.1985.0330310 Published online by Cambridge University Press

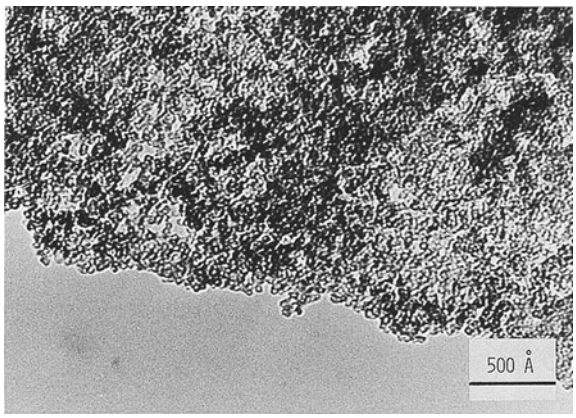


Figure 4. Transmission electron micrograph of allophane (Ki-P) heated at 500°C.

of allophane reflecting its chemical composition and hydration status. The d-spacing of the second band maximum calculated using the Bragg formula increased from 12.3 to 14.5 Å with decreasing SiO_2/Al_2O_3 ratio. The spacing probably indicated the magnitude of size of the domain arising from the ordering.

Comparison of Figures 1 and 3 shows that heating allophane samples at 200°C and equilibrating them at 0% r.h. resulted in the enhancement of the first XRD band relative to the second band. The position of the first band did not change, but its intensity was increased by heating and attained its maximum at 400° to 500°C, suggesting that the dehydroxylated allophane still consisted of spherical particles similar to those found in unheated allophane. This finding is surprising because Henmi and Wada (1976) found that the "hollow" allophane spherical particles broke down very easily in the electron beam, and other workers found that heating caused substantial changes on the infrared spectra of allophane (Kitagawa, 1974; Egashira and Aomine, 1974; Henmi *et al.*, 1981). As illustrated in Figure 4 for the Ki-P sample, however, electron microscopy confirmed that allophane heated at 500°C still consisted of the spherical particles with diameters of 35 to 40 Å. These particles also acquired a stability to a prolonged exposure in the electron beam, and the contrast between the inner parts and the wall of the particle seemed to be enhanced. Thus, some structural changes in allophane appeared to have occurred on dehydroxylation but did not result in the destruction of its framework structure.

The collapse of the second XRD band also proceeded with increasing temperature and was nearly complete at 500°C. A comparison of Figures 1 and 3 shows that equilibrating the heated sample at 100% r.h. regained the second band, particularly for those samples heated at 200° and 300°C. The regaining of the second band was more marked for the PA and VA samples than for the Ki-P and Ku-P samples. These observations confirm that the second XRD band arose from some long-

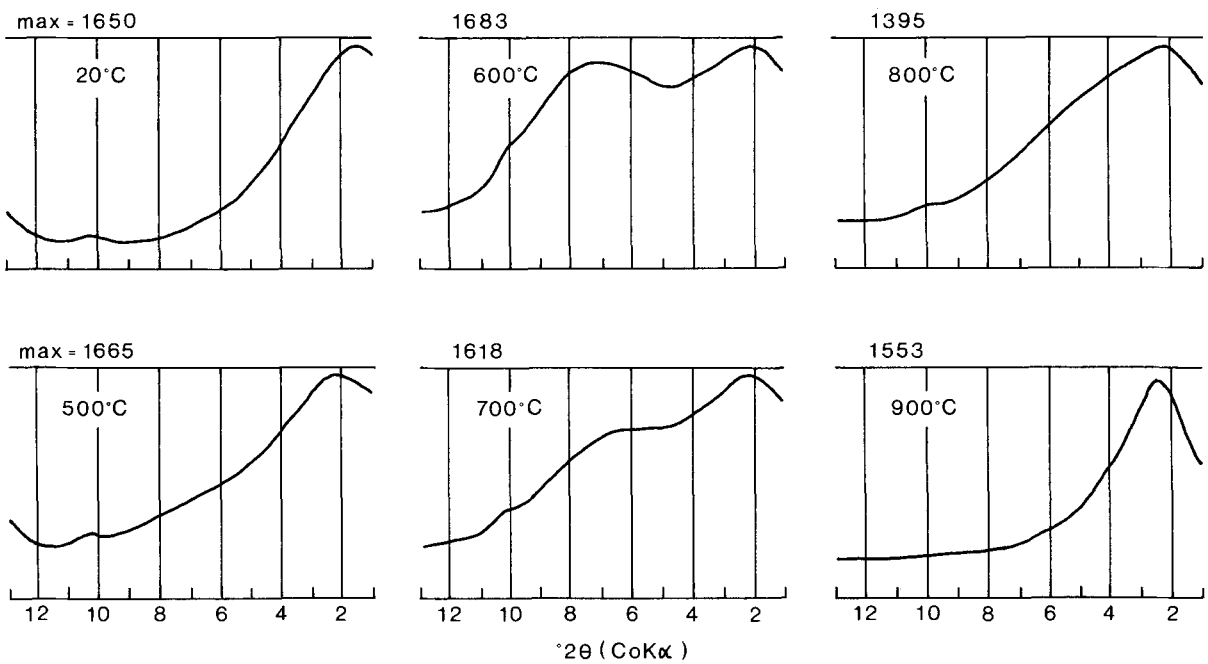


Figure 5. X-ray powder diffraction patterns of kaolinite unheated and heated at 500°, 600°, 700°, 800°, and 900°C. "Max" denotes the maximum count in cps.

https://doi.org/10.1346/CCMN.1985.0330310 Published online by Cambridge University Press

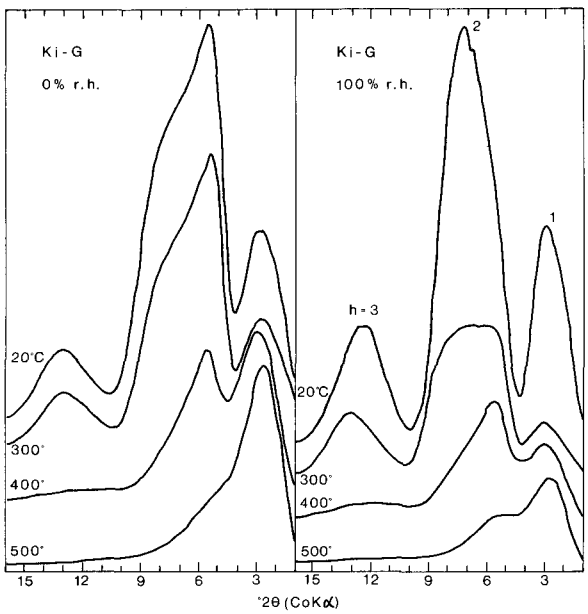


Figure 6. X-ray powder diffraction patterns of imogolite (Ki-G) unheated and heated at 300°, 400°, and 500°C and equilibrated at 0 and 100% relative humidity, respectively.

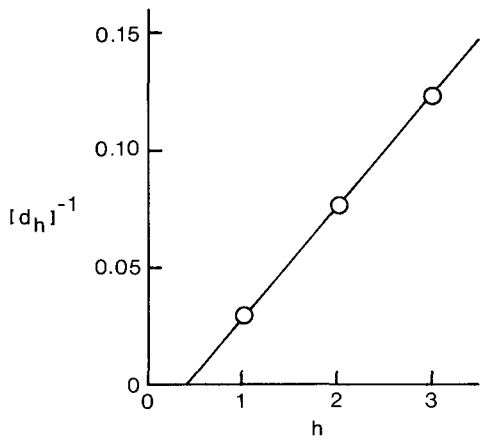


Figure 7. Plot of $[d_h]^{-1}$ vs. h for imogolite (Ki-G). See text for explanation.

range ordering in the structure of allophane that depended on the SiO_2/Al_2O_3 ratio. Thus, water molecules must have had some role in developing the order as structural water.

Also, an XRD band similar to the second band of allophane was obtained for a kaolinite sample dehydroxylated by heating. Figure 5 shows that the band with a maximum at 14.6 Å (7.0°2θ; CoKα) appeared on heating kaolinite at 600°C. The appearance of this XRD band demonstrates the persistence of some long-range order in metakaolin as postulated by Brindley and Nakahira (1959), and its disappearance at higher temperatures possibly denotes the start of the transformation of metakaolin to Al-Si spinel.

Imogolite

Figure 6 shows the XRD patterns of the unheated Ki-G sample at 0 and 100% r.h. Three nearly symmetrical XRD bands with maxima at 2.9, 7.2, and 12.4°2θ (CoKα) are present; the band at 2.9°2θ (d = 30 Å) has not been reported earlier. The 7.2°2θ (d = 12.3 Å) and 12.4°2θ (d = 7.1 Å) bands were indexed as 020 and 030 reflections from the imogolite structure with a *b*-spacing of 23 Å by Cradwick *et al.* (1972). The d-values of the three XRD bands, however, formed an irrational series. At 0% r.h., an additional, relatively sharp maximum developed at 5.5°2θ (d = 18.6 Å), overlapping the second band. This feature was noted for natural (Wada and Yoshinaga, 1969) and synthetic (Farmer and Fraser, 1979) imogolite heated at 100°C.

Vainshtein (1966) showed that several (<7 to 10) cylindrical units aligned to form bundles of varying size gave "non-Bragg XRD maxima" and that their positions were governed solely by the separation between the adjacent units, *a*. The following relationship exists:

$$[d_h]^{-1} = (h + \epsilon)/a,$$

where d_h is the d-spacing of the h*th* XRD maximum and ϵ is a small constant. A plot of $[d_h]^{-1}$ vs. h is shown in Figure 7. The predicted proportionality occurs for imogolite and indicates that a = 22 Å, in agreement with the external diameter of the tube of about 20 Å observed in the electron microscope (Wada *et al.*, 1970). The additional XRD maximum at 5.5°2θ (d = 18.6 Å) at 0% r.h. can be explained by assuming that larger numbers of the tubes were arranged in a hexagonal close-packed arrangement, where the first XRD line with index 111 is predicted to appear at $d = a\sqrt{3}/2$ = 19.1 Å. A similar explanation for the additional band was given by Farmer and Fraser (1979).

Figure 6 also shows the XRD patterns of the Ki-G samples heated at 200° to 500°C. Yoshinaga and Aomine (1962) showed by thermal analyses that the dehydroxylation of imogolite starts at 400°C and ends at 500°C. The XRD patterns shown in Figure 6 also indicate that the destruction of the tube started at 400°C and finished at 500°C. The second and third XRD bands disappeared at 400°C, and the remaining additional band with maximum at 18.6 Å nearly disappeared at 500°C. Only the first band with maximum at about 40 Å remained at 500°C and showed a slight shift toward the low-angle side and a considerable increase in intensity. The electron micrograph of the Ki-G sample heated at 500°C (Figure 8) shows that most tubes broke down and changed to material showing a somewhat granular, poorly defined morphology, though

https://doi.org/10.1346/CCMN.1985.0330310 Published online by Cambridge University Press

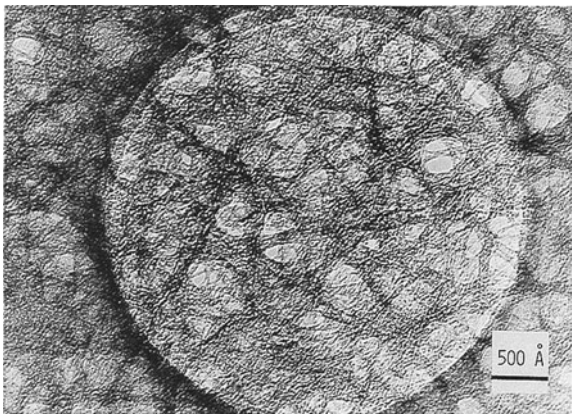


Figure 8. Transmission electron micrograph of imogolite (Ki-G) heated at 500°C.

some structure associated with the arrangement of the tubes remained.

Implications to the structure of allophane

Whether or not the wall of the allophane particle is composed of a defect kaolin (Wada and Wada, 1977) or an imogolite-like (Parfitt *et al.,* 1980; Parfitt and Henmi, 1980) structure has been debated. Wada and Wada (1977) suggested that the wall is made up of one Al-octahedral and one Si(Al)-tetrahedral sheet. On this basis, Wada (1979) proposed structural formulae for two end members of allophane with the SiO_2/Al_2O_3 ratios of 1.0 and 2.0 and suggested that the Si(Al) tetrahedral sheet provides the framework of the allophane structure. Parfitt *et al.* (1980) proposed that the wall of the allophane particle with the SiO_2/Al_2O_3 ratio close to 1.0 is made up of imogolite structural units similar to "proto-imogolite" and suggested that the framework of the allophane structure is an Al-octahedral sheet. They pointed out that the absorption bands at 580 and 680 cm^{-1} on the infrared spectra are common to all allophanes and probably arise from an octahedral sheet similar to the gibbsite sheet present in the imogolite structure. More recently, Si and Al coordination in allophanes with low SiO_2/Al_2O_3 ratios (0.82–1.3) was studied by solid state nuclear magnetic resonance (NMR). Barron *et al.* (1982) found that these allophanes contained only Si-tetrahedra of the imogolite type, and Wilson *et al.* (1984) reported that all Al in one of those allophanes was in six-fold coordination.

The observed differences in the effect of heating on the XRD patterns and morphology between allophane and imogolite suggest that the two minerals are different in the framework structure that maintains their particle form. The destruction of the imogolite tube on dehydroxylation at 400°C conforms with the structure proposed by Cradwick *et al.* (1972) in which the Al-octahedral sheet constitutes the framework of structure. On the other hand, the dehydroxylation of allophane starts at a temperature of less than 400°C (Kitagawa, 1974; Henmi *et al.,* 1981), but "hollow" spherical particles remain unaffected in appearance even at 500° to 600°C irrespective of their SiO_2/Al_2O_3 ratio. These data suggest that the Si or Si(Al) tetrahedral sheet makes up the framework structure of allophane. The stability of the Si-tetrahedral sheet in the kaolin layer in the thermal transformation from kaolinite to metakaolin was postulated by Brindley and Nakahira (1959). Our suggestion contradicts, however, the NMR results by Barron *et al.* (1982) and Wilson *et al.* (1984).

ACKNOWLEDGMENTS

The authors thank A. J. Vaars for technical assistance and Stokvis Chemicalien B. V. for providing the Ludox sample.

REFERENCES

Barron, P. F., Wilson, M. A., Campbell, A. S., and Frost, R. L. (1982) Detection of imogolite in soils using solid state ^{29}Si NMR: *Nature* **299,** 616–618.

Brindley, G. W. and Nakahira, M. (1959) The kaolinite-mullite reaction series. II. Metakaolin: *J. Amer. Ceram. Soc.* **42,** 314–318.

Brown, G. (1980) Associated minerals: in *Crystal Structures of Clay Minerals and Their X-ray Identification,* G. W. Brindley and G. Brown, eds., Mineralogical Society, London, 361–410.

Cradwick, P. D. G., Farmer, V. C., Russell, J. D., Masson, C. R., Wada, K., and Yoshinaga, N. (1972) Imogolite, a hydrated aluminum silicate of tubular structure: *Nature* **240,** 187–189.

Egashira, K. and Aomine, S. (1974) Effects of drying and heating of the surface area of allophane and imogolite: *Clay Sci.* **4,** 231–242.

Farmer, V. C. and Fraser, A. R. (1979) Synthetic imogolite, a tubular hydroxyaluminum silicate: in *Proc. Int. Clay Conf., Oxford, 1978,* M. M. Mortland and V. C. Farmer, eds., Elsevier, Amsterdam, 547–553.

Guinier, A. (1963) *X-ray Diffraction in Crystals, Imperfect Crystals and Amorphous Bodies:* Freeman, San Francisco, 72–74, 340–342.

Henmi, T., Tange, K., Minagawa, T., and Yoshinaga, N. (1981) Effect of SiO_2/R_2O_3 ratio on the thermal reactions of allophane. II. Infrared and X-ray powder diffraction data: *Clays & Clay Minerals* **29,** 124–128.

Henmi, T. and Wada, K. (1976) Morphology and composition of allophane: *Amer. Mineral.* **61,** 379–390.

Kitagawa, Y. (1971) The "unit particle" of allophane: *Amer. Mineral.* **56,** 465–475.

Kitagawa, Y. (1974) Dehydration of allophane and its structural formula: *Amer. Mineral.* **59,** 1094–1098.

MacEwan, D. M. C., Ruiz, A. A., and Brown, G. (1961) Interstratified clay minerals: in *The X-ray Identification and Crystal Structure of Clay Minerals,* G. Brown, ed., Mineralogical Society, London, 393–445.

Parfitt, R. L., Furkert, R. J., and Henmi, T. (1980) Identification and structure of two types of allophane from volcanic ash soils and tephra: *Clays & Clay Minerals* **28,** 328–334.

Parfitt, R. L. and Henmi, T. (1980) Structure of some allophanes from New Zealand: *Clays & Clay Minerals* **28,** 285–294.

https://doi.org/10.1346/CCMN.1985.0330310 Published online by Cambridge University Press

Vainshtein, B. K. (1966) *Diffraction of X-ray by Chain Molecules:* Elsevier, Amsterdam, 328–334.

van der Gaast, S. J. and Vaars, A. J. (1981) A method to eliminate the background in X-ray diffraction patterns of oriented clay mineral samples: *Clay Miner.* **16,** 383–393.

Wada, K. (1979) Structural formulas of allophanes: in *Proc. Int. Clay Conf., Oxford, 1978,* M. M. Mortland and V. C. Farmer, eds., Elsevier, Amsterdam, 537–545.

Wada, K. and Yoshinaga, N. (1969) The structure of "imogolite": *Amer. Mineral.* **54,** 50–71.

Wada, K., Yoshinaga, N., Yotsumoto, H., Ibe, K., and Aida, S. (1970) High resolution electron micrographs of imogolite: *Clay Miner.* **8,** 487–489.

Wada, S. and Wada, K. (1977) Density and structure of allophane: *Clay Miner.* **12,** 289–298.

Wilson, M. A., Barron, P. F., and Campbell, A. S. (1984) Detection of aluminum coordination in soils and clay fractions using ^{27}Al magic angle spinning n.m.r.: *J. Soil Sci.* **35,** 201–207.

Yoshinaga, N. and Aomine, S. (1962) Imogolite in some Ando soils: *Soil Sci. Plant Nutr.* **8,** 22–29.

(Received 4 August 1984; accepted 7 November 1984; Ms. 1389)

https://doi.org/10.1346/CCMN.1985.0330310 Published online by Cambridge University Press